# Temperature-light-dependent JV and TPV analysis of pure sulfide based $Cu_2ZnSnS_4$ solar cells

Zhengfei Wei[1], Adam Pockett[1], James D. Mcgettrick[1], Chung Man Fung[2], Owen J. Guy[2], Matthew J. Carnie[1] and Trystan M. Watson[1]

[1]SPECIFIC, College of Engineering, Swansea University, Bay Campus, Swansea, SA1 8EN
[2]Centre of NanoHealth (CNH), College of Engineering, Swansea University, Singleton Campus, Swansea, SA2 8PP

***Abstract* — In this work, we exploit temperature-light-dependent current-density-voltage (T-JV) and transient photovoltage measurements (T-TPV) to investigate charge dynamics, especially at the back contact, in solution-processed $Cu_2ZnSnS_4$ solar cells. A $Si_xN_y$ hole barrier was grown on top of Mo to help to investigate carrier dynamics. By using T-JV techniques, we are able to observe the dominant recombination mechanism occurring at the back contact interface that could lead to significant open-circuit voltage ($V_{oc}$) loss. In combination with T-TPV, TPV decay time mapping across temperature in a range of 213-313 K and light intensity range of 0.01-1 suns was used to explore interface related recombination and charge transport for CZTS solar cell devices.**

***Index Terms* — CZTS, TPV, T-JV, recombination and solar cell.**

## I. Introduction

Pure sulfide CZTS thin film solar cells have been extensively studied in the last few years as an earth-abundant and environmentally-friendly alternative to well-established CIGS technologies [1-3]. The optimization of the interface between back contact and absorber is one of main challenges to improve the electrical behavior and further enhance solar cell device efficiency. In this work, we present a combination technique of temperature-light-dependent JV and TPV measurement to investigate the charge dynamics of devices using pure sulfide CZTS. A 10 nm-$Si_xN_y$ thin film was introduced as a hole extraction blocking layer to help to identify the dominant recombination path.

## III. Experimental Section

The CZTS layers were deposited on Mo back contacts by spin-coating of C-Z-T-S solution precursors and subsequently sulfurized in a rapid thermal processing (RTP, MTI Corporation) furnace at 560 °C for 20 mins. The solution preparation details are the same as those reported earlier. [4] The thickness of the CZTS absorbers was 1.2-1.3 μm. After coating CZTS layers, a ~70nm thick CdS layer was deposited by chemical bath deposition. Sputtered intrinsic ZnO (~50 nm) and ITO (~350 nm) served as a transparent conductive oxide. A Ni-Al metal grid was deposited using thermal evaporation to improve the conductivity of the device. A 10 nm-thick $Si_xN_y$ layer was deposited through plasma enhanced chemical vapour deposition (PECVD).

UPS was performed alongside XPS in the Kratos Axis Supra, utilising the He(I) line with a pass energy of 10 eV, step size of 0.025 eV and a 65 ms dwell. A 110 $\mu$m aperture was utilised in order to prevent saturation of the detector. The secondary electron cut-off and valence band edges were estimated using the Step Up and Step Down edge backgrounds within CasaXPS. In each case the measured value is the intersection of the step with the background electron counts. The current-density-voltage (J-V) curves for the solar cell devices were measured under simulated AM 1.5G spectrum and 100 mW/cm$^2$ (1 sun) illumination. Transient photovoltage measurements were performed using a commercially available transient measurement system (Automatic Research GmbH). This system uses a 635 nm red laser diode driven by a waveform generator (Keysight 33500B). The laser pulse length was 100 ns. Background illumination was provided by a white LED with its intensity calibrated to generate the same device photocurrent as measured using the solar simulator. This intensity is referred to as 1 Sun equivalent. Transient responses were captured by a digital storage oscilloscope (Keysight DSOX2024A), the number of sample averages being adjusted to optimise signal noise and measurement time. The device under test is assumed to be held at open-circuit by the 1 MΩ oscilloscope input. TPV decays were fitted using a single exponential function. Temperature dependent J-V and TPV measurements were performed using a temperature-controlled chamber (Linkam) under liquid nitrogen cooling.

## III. results And Discussion

A 30nm-Mo-capping/$Si_xN_y$/Mo/SLG stack was used to fabricate CZTS devices and compare against the reference CZTS device directly deposited onto Mo/SLG. Unfortunately, most devices with Mo/$Si_xN_y$ back contact showed a significant reduction on open-circuit voltage and short-circuit current. The highest efficiency of 1.99% was achieved with Mo-30 nm/$Si_xN_y$ barrier layer with significant reduction on the $V_{oc}$ and $J_{sc}$ along with some decrease in FF as compared to solar

978-1-5386-8529-7/18/$31.00 ©2018 IEEE

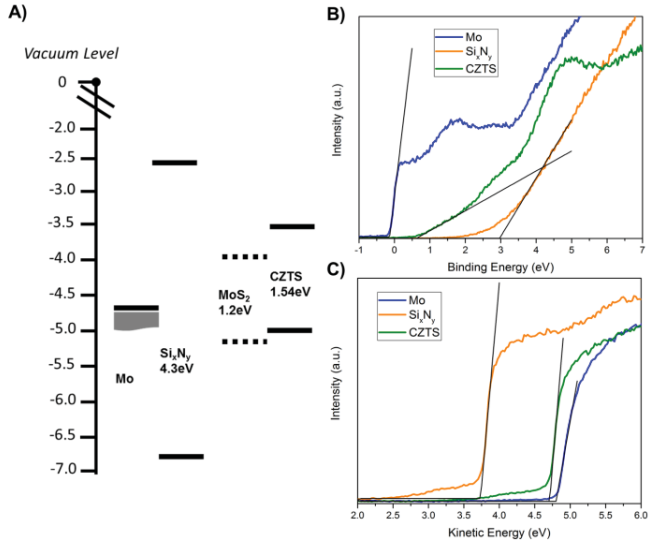


Fig. 1. A) Band diagram of the effective band edge states of the CZTS and modified back contact layers in solid lines. B) the Fermi level and C) work functions are measured by UPS which were used to calculate the ionisation potential (or valence band maximum) of each film. The band gap of the CZTS and $Si_xN_y$ were obtained using EQE and UV-VIS, respectively. Band edge states of the $MoS_2$ were adapted from reference [5], which could not be detected by UPS in this work.

cells without barrier layers

To investigate differences in energetics after applying the $Mo/Si_xN_y$ barrier layers, we employed ultraviolet photoelectron spectroscopy (UPS). Ionisation potentials (IP or valence band maximum of (6.8 ± 0.1) eV and (5.1 ± 0.1) eV were measured for $Si_xN_y$ and CZTS films, respectively, as shown in Figure 1. Mo thin films were found to have a work function of (4.7 ± 0.1) eV. A 2 eV greater barrier height was introduced by 30 nm-thick $Mo/Si_xN_y$ layers compared to unmodified CZTS. This difference would form a blocking back contact at the interface between the Mo and CZTS, which can suppress the majority carrier (hole) transport.

To further investigate the deficiency of the performance of the CZTS device with a $Mo/Si_xN_y$ barrier as compared with the CZTS device without this barrier, temperature dependent $V_{oc}$ data has been collected to determine the dominant recombination processes. The relationship between $V_{oc}$ and temperature is according to [6] and as shown below

$$V_{OC} \equiv \frac{E_a}{q} - \frac{AkT}{q}\ln\left(\frac{J_{00}}{J_L}\right) \qquad (1)$$

where $E_a$, $A$, $J_{00}$, $J_L$, $q$, $k$ and $T$ are the activation energy for dominant recombination mechanism, diode ideality factor, reverse saturation current prefactor, photocurrent, electron charge, Boltzmann constant and the temperature, respectively. The $V_{oc}$ vs $T$ plots are shown in Figure 2A for the CZTS

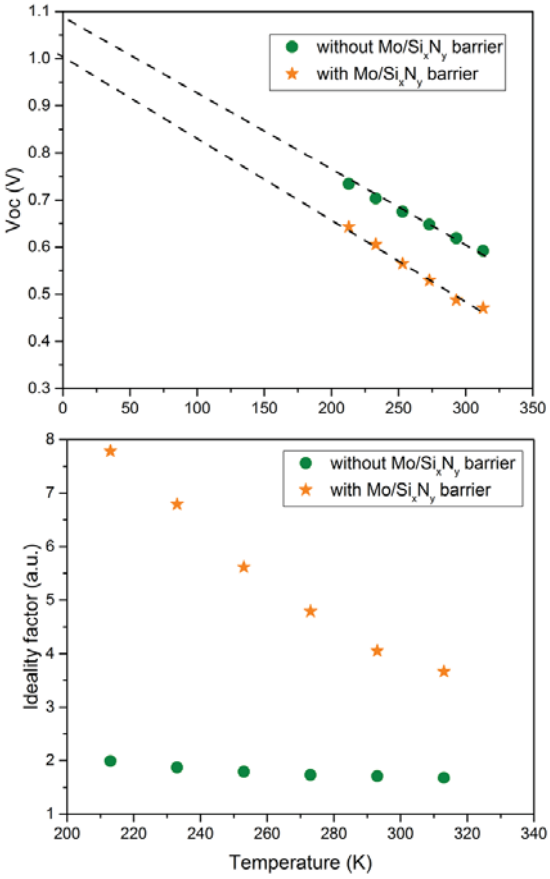


Fig. 2. A) Temperature dependency of open-circuit voltage (Voc) for CZTS solar cells without $Mo/Si_xN_y$ barrier layers (solid circles) and with $Mo/Si_xN_y$ barrier layers (solid stars), the linear extrapolation to T = 0 K in dashed lines. Data for both devices have 0 K intercepts that do not reach the band gap value. B) The correlated ideality factors versus temperature data for without $Mo/Si_xN_y$ barrier layers (solid circles) and with $Mo/Si_xN_y$ barrier layers (solid stars).

devices with and without $Mo/Si_xN_y$ barrier layers, which yield 0 K intercept of the linear extrapolation of $E_a/q$ values of 1.01 and 1.09 eV, respectively. Those $E_a/q$ values are low compared to their respective band gap values (1.54 and 1.47eV) obtained from EQE measurement. This result indicates that the main recombination mechanism in these CZTS cells is dominated by interface recombination.[7] The more pronounced reduction on $E_a/q$ value of the CZTS cell with the $Mo/Si_xN_y$ barrier layers could be due to increased interface recombination occurring at the back contact with improper band alignment (Figure 1A). The efficiency for both devices collapses at low temperature due to increasing series resistance and the possible charge carrier freeze-out effect at low temperature as agreed with other publications.[7, 8] In Figure 2B, the T-dependent diode ideality factors for both CZTS solar cells with and without $Mo/Si_xN_y$ barrier layers were plotted. The diode ideality factors for the CZTS solar cell

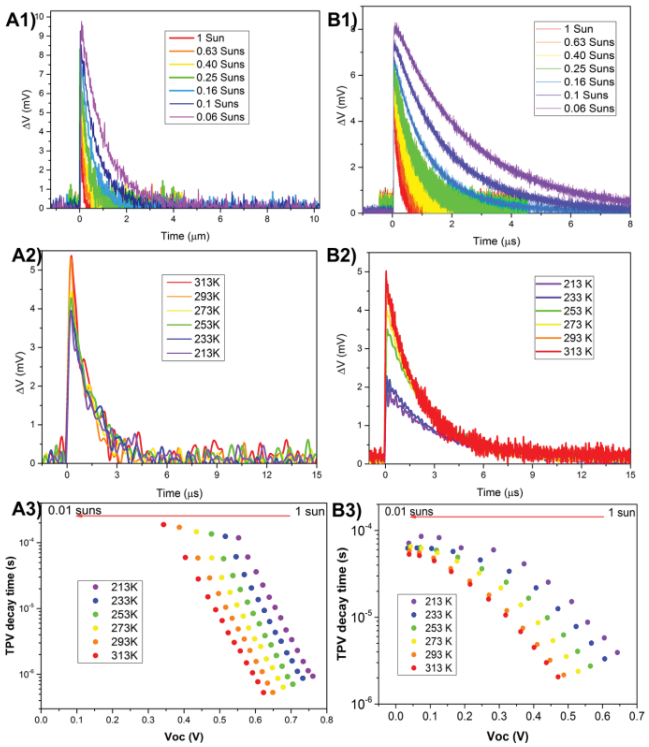


F ig. 3. The representative TPV decays analysis of CZTS solar cells without Mo/$Si_xN_y$ barrier layers (A) and with Mo/$Si_xN_y$ barrier layers (B). A1) and B1) The representative TPV decay as a function of white-light bias in the range of 0.06 - 1 suns at 293 K. A2) and B2) Temperature-dependent TPV decay under 1 sun white-light bias at the temperature range of 213 – 313 K. A3) and B3) TPV decay time characteristics of CZTS solar cells under WLB range of 0.01 – 1 suns and temperature range of 213 – 313 K.

without the Mo/$Si_xN_y$ barrier are between 1 and 2, and showing a marginal variation in the measured temperature range, which could be an indication of the deep defects acting as dominant trap states or so called Shockley-Read-Hall recombination via band tails.[9, 10] However, a significant increase of diode ideality factor (>2) was observed for CZTS solar cells with the Mo/$Si_xN_y$ barrier at low temperatures. The origin of $A$>2 is not possible by considering a single recombination routes, involving a multistep recombination process via a series of trap states distributed within the solar cell device structure. [11] This would indicate strong back contact recombination which could lower $V_{oc}$.[7, 11, 12]

To understand how the charges transport behaviour at the CZTS/back contact interface differs between the device types, we conducted temperature-dependent TPV measurements. For TPV measurements, a light pulse is applied to a device held at open-circuit condition under a white-light bias (WLB), and the resulting photovoltage changes created by the laser pulse ($\Delta V$) is measured over time. From this, we measured the decay time of the open-circuit voltage as a function of the intensity of WLB as shown in Figure 3A1 and 3B1. TPV decay measurement gives insight into the internal recombination dynamics of the charge carriers. The decay time represents the total extraction time of the charge carriers before they recombine or are trapped in the defects.[13] The longer decay time measured, the higher chance the photo-generated charge carriers can be extracted. The decay times of charge carriers for the CZTS solar cells with and without Mo/$Si_xN_y$ barrier layers are estimated on the order of ~μs in the WLB range of 0.06 – 1 suns. With increasing WLB, $V_{oc}$ of both CZTS devices increases. This could be caused by shallow defects were fulfilled with photo-excited carriers at higher excitation densities.[14] By increasing the WLB, there are more photo-generated minority charge carriers (electrons) in the CZTS absorber which could also increase the internal recombination with holes, reducing the extraction time. The variation on decay time of CZTS with Mo/$Si_xN_y$ barrier layers using different light intensities is more significant than CZTS device without the Mo/$Si_xN_y$ barrier layers. This would be a sign of stronger recombination caused by this modified back contact. To investigate the thermally activated charge transport, temperature dependent Figure 3A2 and 3b2 show the TPV decay for the CZTS solar cells with and without Mo/$Si_xN_y$ barrier layers at different temperature under 1 sun WLB. The decay time of both CZTS devices increases with decreasing temperature. The longer extraction time could be due to reduced thermal energy to assist the charge carrier to jump spatially over fluctuated electrostatic potential [15] and travel across the CZTS device. A more pronounced reduction on $\Delta V$ and decay time for CZTS device with Mo/$Si_xN_y$ barrier layers at different temperature as compared to the CZTS device without the barrier layers was obtained. To find out the combined effects of the intensity of WLB and temperature on TPV decay time, TPV decay time versus $V_{oc}$ at different conditions were shown in Figure 3A3 and 3B3. The data were recorded until almost lost $V_{oc}$ at lowest light levels of WLB. We could still obtain $V_{oc}$ at light intensity level less than 0.01 suns for CZTS solar cell device without Mo/$Si_xN_y$ barrier layers. In other words, the increase interfacial recombination in the cell with Mo/SiN causes a significant decrease in $V_{oc}$ at low light intensities. The TPV signal decays 100 times faster after introducing the Mo/$Si_xN_y$ barrier into device structure. These results indicate that the recombination within the CZTS device with Mo/$Si_xN_y$ barrier layers may not only account for trapping and detrapping process[16], and can thus be attributed to the increased interface recombination between accumulated holes near the high barrier layer and free electrons in CZTS. This is in good agreement with the hole blocking effect obtained from temperature dependent $J$-$V$ measurement.

## V. Conclusion

In conclusion, the interface recombination was determined as the dominate recombination path in the deposited CZTS

solar cells using T-JV measurement. A Mo/$Si_xN_y$ barrier layers were used as a hole extraction blocking layer to help to identify the dominant recombination path. Temperature dependent J-V and TPV showed the increased interface recombination and poor hole extraction due to misalignment of band edges between Mo/$Si_xN_y$/CZTS region.

## VI. Acknowledgements

This work was funded by Engineering and Science Research Council (EPSRC): EP/L017792/1: Photovoltaic Technology Based on Earth-Abundant materials (PVTeam). A. P. and M. J. C. thank: the British Council for funding, through the Newton Al-Farabi Partnership; and the European Regional Development Fund (ERDF) and the Welsh European Funding Office (WEFO) for funding the 2nd Solar Photovoltaic Academic Research Consortium (SPARC II).

## References

[1] C. Yan, K. Sun, J. Huang, S. Johnston, F. Liu, B. P. Veettil, *et al.*, "Beyond 11% Efficient Sulfide Kesterite Cu2ZnxCd1−xSnS4 Solar Cell: Effects of Cadmium Alloying," *ACS Energy Letters,* vol. 2, pp. 930-936, 2017/04/14 2017.

[2] Z. Su, J. M. R. Tan, X. Li, X. Zeng, S. K. Batabyal, and L. H. Wong, "Cation Substitution of Solution-Processed Cu2ZnSnS4 Thin Film Solar Cell with over 9% Efficiency," *Advanced Energy Materials,* vol. 5, pp. 1500682-n/a, 2015.

[3] T. Ericson, F. Larsson, T. Törndahl, C. Frisk, J. Larsen, V. Kosyak, *et al.*, "Zinc-Tin-Oxide Buffer Layer and Low Temperature Post Annealing Resulting in a 9.0% Efficient Cd-Free Cu2ZnSnS4 Solar Cell," *Solar RRL,* vol. 1, pp. 1700001-n/a, 2017.

[4] Z. Wei, M. Zhu, J. D. McGettrick, G. P. Kissling, L. M. Peter, and T. M. Watson, "The effect of additional sulfur on solution-processed pure sulfide Cu2ZnSnS4 solar cell absorber layers," *MRS Advances,* vol. FirstView, pp. 1-6, 2016.

[5] T. P. Dhakal, S. Harvey, M. van Hest, and G. Teeter, "Back Contact Band Offset Study of Mo-CZTS Based Solar Cell Structure by Using XPS/UPS Techniques," presented at the 2015 IEEE 42nd Photovoltaic Specialist Conference (PVSC), New Orleans, 2015.

[6] V. Nadenau, U. Rau, A. Jasenek, and H. W. Schock, "Electronic properties of CuGaSe2-based heterojunction solar cells. Part I. Transport analysis," *Journal of Applied Physics,* vol. 87, pp. 584-593, 2000.

[7] D. B. Mitzi, O. Gunawan, T. K. Todorov, K. Wang, and S. Guha, "The path towards a high-performance solution-processed kesterite solar cell," *Solar Energy Materials and Solar Cells,* vol. 95, pp. 1421-1436, 2011/06/01/ 2011.

[8] T. K. Todorov, J. Tang, S. Bag, O. Gunawan, T. Gokmen, Y. Zhu, *et al.*, "Beyond 11% Efficiency: Characteristics of State-of-the-Art Cu2ZnSn(S,Se)4 Solar Cells," *Advanced Energy Materials,* vol. 3, pp. 34-38, 2013.

[9] S. S. Hegedus and W. N. Shafarman, "Thin-film solar cells: device measurements and analysis," *Progress in Photovoltaics: Research and Applications,* vol. 12, pp. 155-176, 2004.

[10] C. v. Berkel, M. J. Powell, A. R. Franklin, and I. D. French, "Quality factor in a ‐ Si:H nip and pin diodes," *Journal of Applied Physics,* vol. 73, pp. 5264-5268, 1993.

[11] U. Rau, "Tunneling-enhanced recombination in Cu(In,Ga)Se2 heterojunction solar cells," *Applied Physics Letters,* vol. 74, pp. 111-113, 1999.

[12] O. Gunawan, T. Gokmen, and D. B. Mitzi, "Suns-VOC characteristics of high performance kesterite solar cells," *Journal of Applied Physics,* vol. 116, p. 084504, 2014.

[13] W. M. M. Lin, D. Bozyigit, O. Yarema, and V. Wood, "Transient Photovoltage Measurements in Nanocrystal-Based Solar Cells," *The Journal of Physical Chemistry C,* vol. 120, pp. 12900-12908, 2016/06/16 2016.

[14] J. E. Halpert, F. S. F. Morgenstern, B. Ehrler, Y. Vaynzof, D. Credgington, and N. C. Greenham, "Charge Dynamics in Solution-Processed Nanocrystalline CuInS2 Solar Cells," *ACS Nano,* vol. 9, pp. 5857-5867, 2015/06/23 2015.

[15] T. Gokmen, O. Gunawan, T. K. Todorov, and D. B. Mitzi, "Band tailing and efficiency limitation in kesterite solar cells," *Applied Physics Letters,* vol. 103, p. 103506, 2013.

[16] C. J. Hages, A. Redinger, S. Levcenko, H. Hempel, M. J. Koeper, R. Agrawal, *et al.*, "Identifying the Real Minority Carrier Lifetime in Nonideal Semiconductors: A Case Study of Kesterite Materials," *Advanced Energy Materials,* vol. 7, pp. 1700167-n/a, 2017.